

# Polyazeotropic Behavior in the Binary System 1,1,1,2,3,4,4,5,5,5-Decafluoropentane + Oxolane

Sonia Loras,<sup>\*,†</sup> Antonio Aucejo,<sup>†</sup> Juan B. Montón,<sup>†</sup> Jaime Wisniak,<sup>‡</sup> and Hugo Segura<sup>§</sup>

Departamento de Ingeniería Química, Facultad de Química, Universitat de Valencia, 46100 Burjassot, Valencia, Spain, and Department of Chemical Engineering, Ben-Gurion University of the Negev, Beer-Sheva, Israel 84105, and Department of Chemical Engineering, Universidad de Concepción, Concepción, Chile

Vapor–liquid equilibrium data at (26.68, 35, and 55) kPa over the whole concentration range and vapor–liquid equilibria at (23 and 45) kPa over a partial concentration range have been determined for the binary system 1,1,1,2,3,4,4,5,5,5-decafluoropentane (HFC-4310mee) + oxolane (THF), in the temperature range (294 to 322) K. Pure component vapor pressures of each constituent have also been measured in the range of boiling temperatures of the mixture. Depending on the concentration range, the system exhibits positive and negative deviations from ideal behavior. Two azeotropes, rich in oxolane and with opposite deviations, have been found both at (23, 26.68, and 35) kPa, while no azeotrope appears at (45 and 55) kPa. According to these results, polyazeotropic behavior ends in a tangent azeotrope as the pressure increases. The vapor–liquid equilibrium data of the solutions were correlated with the mole fraction by the Redlich–Kister equation.

## Introduction

Polyazeotropic behavior in binary systems was discovered experimentally by Gaw and Swinton<sup>1</sup> for the system benzene + hexafluorobenzene. Since then binary polyazeotropy has been reported experimentally for the six organic systems diethylamine + methanol,<sup>2,3</sup> benzene + hexafluorobenzene,<sup>4</sup> 1,2-epoxybutane + methyl ethanoate,<sup>5</sup> ethanoic acid + 2-methylpropyl ethanoate,<sup>6,7</sup> ammonia + 1,1-difluoro-2,2,2-trifluoroethane,<sup>8</sup> and 1,1,1,2,3,4,4,5,5,5-decafluoropentane + oxolane.<sup>9</sup> For the system 1,2-epoxybutane + methyl ethanoate, no azeotropic behavior was found by Montón et al.,<sup>10</sup> who claimed that azeotropy was erroneously detected in ref 5 because of the impurity of the reagents and due to experimental errors. The thermodynamic aspects of azeotropy and polyazeotropy for associating and nonassociating mixtures at low pressures have been discussed in depth by Wisniak et al.<sup>11</sup> and Segura et al.<sup>12</sup> Furthermore, polyazeotropic behavior is predicted by the van der Waals (and van der Waals-type) equations of state, as discussed by van Konynenburg and Scott<sup>13</sup> and by Segura et al.,<sup>14</sup> when the constituent molecules have different sizes. All the experimental and theoretical evidence points to the fact that polyazeotropy, in organic systems, can be attributed to simultaneous positive and negative deviations from ideal behavior, in constrained ranges where the vapor pressures of pure components are of similar order of magnitude.

Azeotropic mixtures of decafluoropentane with many different compounds have been widely patented as solvents, aerosol propellants, heat transfer fluids, blowing agents, polymerization media, carrier fluids, gaseous dielectrics, and power cycle working fluids (see for example refs 15–17). Phase equilibrium data of polyazeotropic mixtures are important for establishing the pattern in which the mul-

**Table 1. Mole % GLC Purities (mass %), Densities, and Normal Boiling Points,  $T_b$ , of HFC-4310mee and THF**

component	purity/mass %	$\rho/\text{kg}\cdot\text{m}^{-3}$	$T_b/\text{K}$
HFC-4310mee (99.9)	99.9	1581.62 <sup>a</sup>	326.85 <sup>a</sup>
THF (99.9)	99.9	881.72 <sup>a</sup>	338.96 <sup>a</sup>
		881.91 <sup>b</sup>	339.08 <sup>c</sup>

<sup>a</sup> Measured. <sup>b</sup> Ramkumar and Kudchadker.<sup>29</sup> <sup>c</sup> Wu and Sandler.<sup>22</sup>

tiple azeotropes evolve with temperature or pressure. The experimental information available allows testing of theories and predictions about polyazeotropic behavior. Equilibrium boiling temperatures and liquid-phase mole fractions for the system 1,1,1,2,3,4,4,5,5,5-decafluoropentane (HFC-4310mee) + oxolane (THF) have been reported by Kao et al.,<sup>9</sup> at 323.18 K and at (26.68 and 58.58) kPa. According to their data, two stationary points of the boiling temperature curve were found at 26.68 kPa, in the range of concentrated THF, pointing to polyazeotropic behavior. No stationary points of the boiling temperature curve were found at 323.15 K and at 58.58 kPa, suggesting that azeotropic behavior disappears as temperature or pressure increases. The data of Kao et al. were measured in a static cell and in an ebulliometer, where no direct measurement of the equilibrium vapor phase concentration is possible. In addition, the vapor pressure data for HFC-4310mee, as measured in the static cell, are in disagreement with the vapor pressure data for the same component, as determined by ebulliometry. The present work was undertaken to measure complete vapor–liquid equilibria (VLE) data for the title system, including vapor pressures of pure components, to characterize the topology of the polyazeotropic behavior.

## Experimental Section

**Chemicals.** THF (99.9 mass %, anhydrous) was purchased from Aldrich Ltd., and HFC-4310mee (99.9 mass %) was donated by DuPont. THF and HFC-4310mee were

\* Corresponding author. E-mail: Sonia.Loras@uv.es.

<sup>†</sup> Universitat de Valencia.

<sup>‡</sup> Ben-Gurion University of the Negev.

<sup>§</sup> Universidad de Concepción.

**Table 2. Experimental Vapor–Liquid Equilibrium Data for HFC-4310mcc (1) + THF (2)**

<i>T</i> /K	<i>x</i> <sub>1</sub>	<i>y</i> <sub>1</sub>	$\gamma_1$	$\gamma_2$	<i>T</i> /K	<i>x</i> <sub>1</sub>	<i>y</i> <sub>1</sub>	$\gamma_1$	$\gamma_2$
23.00 kPa									
299.64	0.000	0.000		1.000	299.85	0.180	0.159	0.594	1.016
299.65	0.028	0.027	0.677	0.999	299.95	0.209	0.189	0.607	1.011
299.65	0.066	0.061	0.629	1.004	300.15	0.238	0.220	0.615	1.001
299.65	0.092	0.082	0.606	1.010	300.25	0.267	0.253	0.629	0.991
299.75	0.123	0.109	0.600	1.011	300.25	0.297	0.292	0.652	0.980
299.85	0.153	0.134	0.592	1.012	300.25	0.327	0.332	0.673	0.966
26.68 kPa									
303.08	0.000	0.000		1.000	302.75	0.437	0.502	0.789	0.898
303.05	0.028	0.029	0.705	1.000	302.45	0.468	0.544	0.811	0.880
303.05	0.057	0.056	0.667	1.003	302.15	0.496	0.591	0.841	0.845
303.05	0.086	0.081	0.637	1.007	301.35	0.563	0.682	0.885	0.785
303.05	0.117	0.106	0.617	1.014	299.95	0.639	0.774	0.943	0.716
303.15	0.147	0.134	0.614	1.013	298.35	0.735	0.844	0.961	0.720
303.35	0.186	0.169	0.609	1.009	297.65	0.776	0.882	0.981	0.668
303.45	0.242	0.228	0.629	1.003	296.55	0.854	0.925	0.983	0.684
303.45	0.296	0.297	0.670	0.983	296.15	0.885	0.946	0.987	0.642
303.45	0.366	0.393	0.717	0.942	295.55	0.927	0.963	0.987	0.709
303.25	0.393	0.438	0.751	0.919	294.95	0.972	0.987	0.992	0.649
303.05	0.419	0.477	0.774	0.901	294.45	1.000	1.000	1.000	
35.00 kPa									
309.65	0.000	0.000		1.000	308.45	0.486	0.576	0.839	0.867
309.55	0.022	0.026	0.777	1.001	307.75	0.535	0.642	0.876	0.830
309.45	0.051	0.055	0.724	1.005	307.05	0.581	0.692	0.894	0.816
309.35	0.088	0.087	0.679	1.013	306.45	0.624	0.740	0.913	0.789
309.35	0.123	0.119	0.661	1.017	305.65	0.665	0.775	0.928	0.792
309.55	0.164	0.157	0.646	1.013	304.85	0.714	0.838	0.967	0.691
309.55	0.217	0.202	0.630	1.023	303.95	0.771	0.873	0.969	0.704
309.45	0.244	0.232	0.647	1.023	303.15	0.818	0.916	0.992	0.608
309.45	0.273	0.275	0.684	1.005	302.35	0.866	0.937	0.994	0.634
309.45	0.348	0.369	0.720	0.976	301.45	0.920	0.968	1.006	0.558
309.15	0.393	0.430	0.752	0.958	300.75	0.975	0.990	1.001	0.558
308.95	0.443	0.503	0.786	0.919	300.42	1.000	1.000	1.000	
45.00 kPa									
316.04	0.000	0.000		1.000	315.55	0.184	0.186	0.688	1.017
315.85	0.033	0.040	0.807	1.000	315.55	0.217	0.218	0.684	1.018
315.65	0.058	0.066	0.771	1.007	315.55	0.248	0.256	0.705	1.008
315.65	0.088	0.094	0.720	1.009	315.45	0.281	0.290	0.706	1.010
315.55	0.118	0.122	0.705	1.014	315.35	0.309	0.328	0.729	0.999
315.55	0.150	0.154	0.699	1.014					
55.00 kPa									
321.36	0.000	0.000		1.000	319.65	0.427	0.498	0.829	0.934
321.25	0.027	0.034	0.842	0.997	319.15	0.481	0.566	0.852	0.908
321.05	0.056	0.067	0.806	1.000	318.45	0.534	0.632	0.881	0.880
320.95	0.086	0.096	0.755	1.004	317.75	0.585	0.705	0.921	0.814
320.85	0.123	0.133	0.734	1.008	316.95	0.628	0.743	0.933	0.815
320.75	0.154	0.161	0.712	1.014	315.85	0.695	0.804	0.953	0.791
320.65	0.180	0.189	0.718	1.015	314.85	0.751	0.861	0.982	0.714
320.65	0.212	0.221	0.713	1.015	314.05	0.806	0.896	0.984	0.708
320.65	0.240	0.253	0.721	1.009	313.25	0.849	0.929	1.000	0.640
320.55	0.270	0.283	0.720	1.012	312.45	0.901	0.956	1.001	0.625
320.35	0.333	0.368	0.764	0.984	311.45	0.964	0.985	1.004	0.609
320.05	0.380	0.425	0.783	0.974	311.02	1.000	1.000	1.000	

used without further purification after chromatography failed to show any significant impurities. The densities and refractive indexes of pure liquids were measured at 298.15 K using an Anton Paar DMA 55 densimeter and an Abbe refractometer Atago 3T, respectively. Temperature was controlled to  $\pm 0.01$  K with a thermostated bath. The uncertainties in density and refractive index measurements are  $\pm 0.01 \text{ kg}\cdot\text{m}^{-3}$  and  $\pm 2 \times 10^{-4}$ , respectively. The experimental values of these properties and the boiling points are given in Table 1 together with those values given in the literature when available.

**Apparatus and Procedure.** An all glass Fischer LA-BODEST vapor–liquid equilibrium apparatus model 602/D, manufactured by Fischer Labor und Verfahrenstechnik (Germany), was used in the equilibrium determinations. The equilibrium vessel was a dynamic recirculating still, equipped with a Cottrell circulation pump. The still is capable of handling pressures from (0.25 to 400) kPa, and

temperatures up to 523 K. The Cottrell pump ensures that both liquid and vapor phases are in intimate contact during boiling and also in contact with the temperature sensing element. The equilibrium temperature was measured with a digital Fischer thermometer with an accuracy of  $\pm 0.1$  K. The apparatus is equipped with two digital pressure sensors: one for the low-pressure region with an accuracy of  $\pm 0.01$  kPa, and another for the high-pressure region with an accuracy of  $\pm 0.1$  kPa. The temperature probe was calibrated against the ice and steam points of distilled water. The manometers were calibrated using the vapor pressure of ultrapure water. The still was operated under constant pressure until equilibrium was reached. Equilibrium conditions were assumed when constant temperature and pressure were obtained for 30 min or longer. Then, samples of liquid and condensate were taken for analysis. The sample extractions were carried out with special syringes that allowed one to withdraw small volume

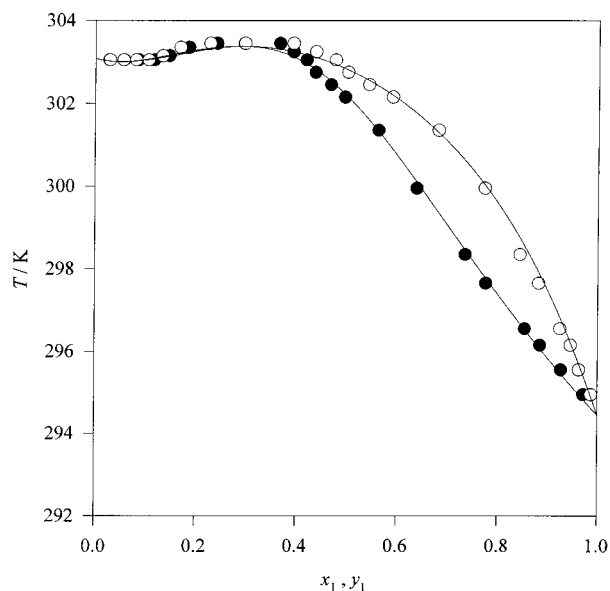


**Figure 1.** Boiling temperature diagram for the system HFC-4310mee (1) + THF (2) at 26.68 kPa: (●) liquid phase mole fraction; (○) vapor phase mole fraction; (---) predicted by eq 4.

samples (0.1 mL) in a system under partial vacuum conditions.

**Analysis.** The concentrations of the liquid and condensed phases were determined using a CE Instruments GC 8000 Top gas chromatograph, after calibration with gravimetrically prepared standard solutions. A flame ionization detector was used together with a 30 m, 0.454 mm i.d. capillary column DB-MTBE (J & W Scientific). The gas chromatography (GC) response peaks were treated with Chrom-Card for Windows, version 1.21. Column, injector, and detector temperatures were 373, 498, and 523 K. Very good separation of peaks was achieved under these conditions, and calibration analyses were carried out to convert the peak area ratios to the mass composition of the sample. The estimated uncertainty in the mole fraction is  $\pm 1 \times 10^{-3}$  from results of the calibration analyses.

## Results

The temperature  $T$  and liquid-phase  $x$  and vapor-phase  $y$  mole fraction measurements at  $P = (23.00, 26.68, 35.00, 45.00, \text{ and } 55.00)$  kPa are reported in Table 2 and in Figures 1–6. Just partial concentration range VLE data have been determined at 23.00 kPa and 45.00 kPa in order to get a better definition of the azeotropic behavior. The indicated table and figures also report the activity coefficients  $\gamma_i$  that were calculated from the following equation:<sup>18</sup>

$$\gamma_i = \frac{y_i P}{x_i P_i^\circ} \quad (1)$$

where  $P$  is the total pressure and  $P_i^\circ$  is the pure component vapor pressure. In eq 1 the vapor phase is assumed to be an ideal gas and the pressure dependence of the liquid-phase fugacity is neglected. Equation 1 was selected to calculate activity coefficients because the low pressures observed in the present VLE data make these simplifications reasonable. In addition, scarce physical information is available for HFC-4310mee, so that an accurate estimation of the second virial coefficients of this component and its mixtures is not possible. However, it should be pointed out that, according to the data of Tripp and Dunlap<sup>19</sup> for

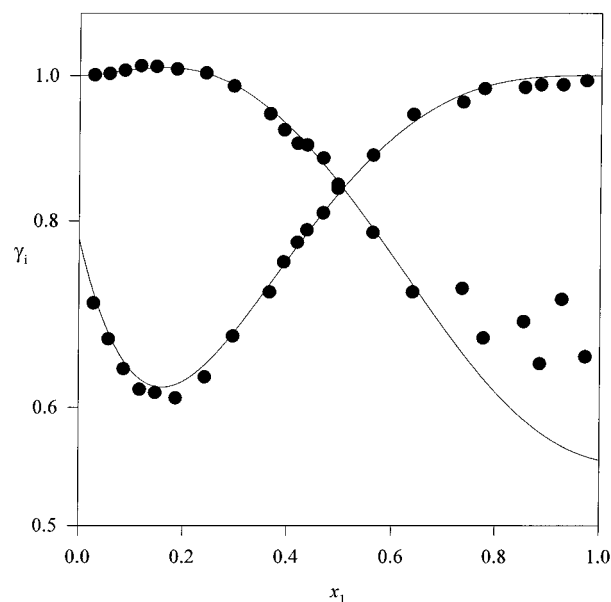


**Figure 2.** Activity coefficients for the system HFC-4310mee (1) + THF (2) at 26.68 kPa: (●)  $\gamma_1^{\text{exptl}}$ ,  $\gamma_2^{\text{exptl}}$ ; (---) predicted by eq 4.

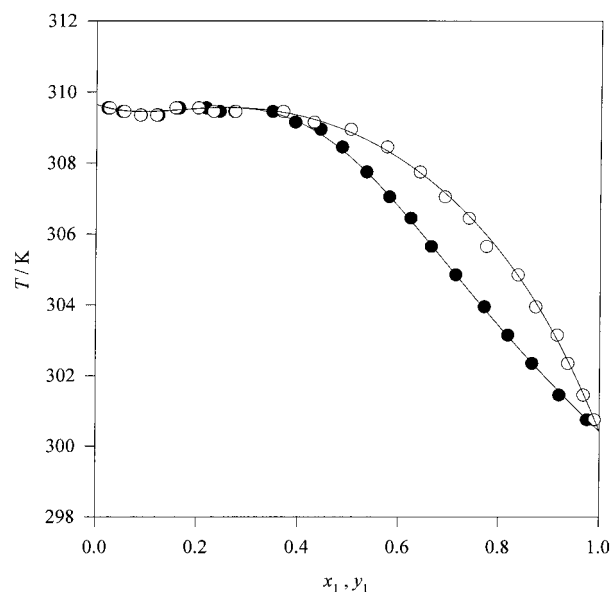


**Figure 3.** Boiling temperature diagram for the system HFC-4310mee (1) + THF (2) at 35.00 kPa: (●) liquid phase mole fraction; (○) vapor phase mole fraction; (---) predicted by eq 4.

decafluorobutane and Garner and McCoubrey<sup>20</sup> for dodecafluoropentane, it is possible to estimate that the order of magnitude of the second virial coefficient of HFC-4310mee at 300 K is  $-1000 \text{ cm}^3 \cdot \text{mol}^{-1}$ . A similar value has been reported by Hossenlopp and Scott<sup>21</sup> for THF. From these values it follows that the error related to the approximation of the vapor-phase fugacity by means of ideal gas relations is on the order of 2% for the present data.

The pure component vapor pressures  $P_i^\circ$  for HFC-4310mee and THF were determined experimentally as a function of the temperature using the same equipment as that for obtaining the VLE data, and pertinent results are presented in Table 3. The measured vapor pressures were correlated using the Antoine equation:

$$\log(P_i^\circ/\text{kPa}) = A_i - \frac{B_i}{(TK) - C_i} \quad (2)$$

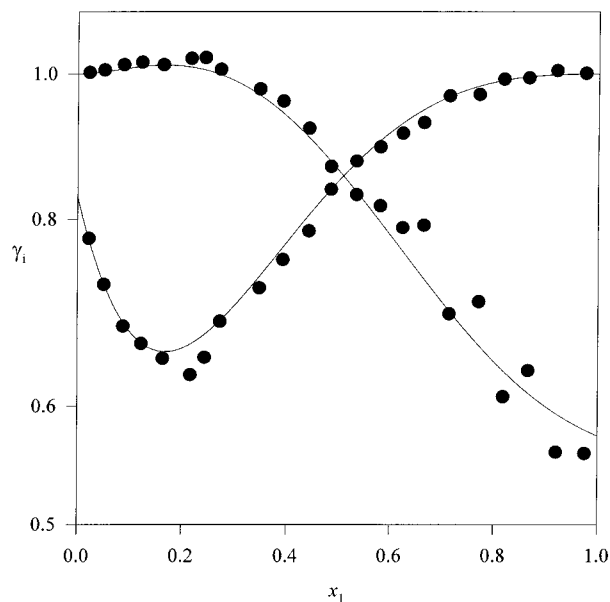


**Figure 4.** Activity coefficients for the system HFC-4310mee (1) + THF (2) at 35.00 kPa: (●)  $\gamma_1^{\text{exptl}}$ ,  $\gamma_2^{\text{exptl}}$ ; (—) predicted by eq 4.

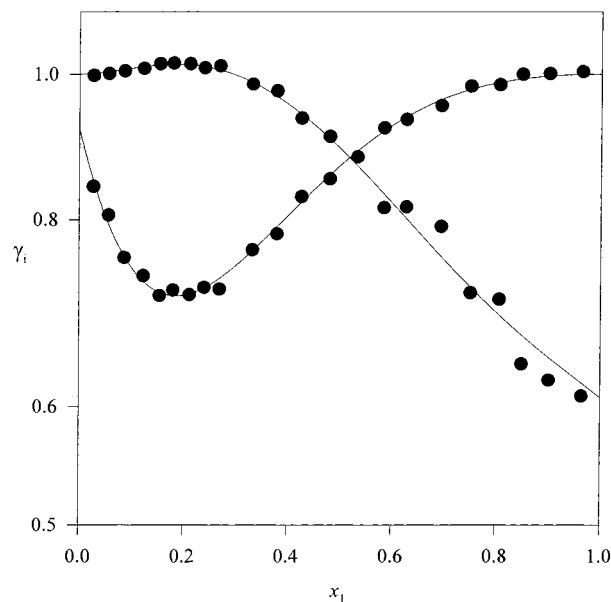


**Figure 6.** Activity coefficients for the system HFC-4310mee (1) + THF (2) at 55.00 kPa: (●)  $\gamma_1^{\text{exptl}}$ ,  $\gamma_2^{\text{exptl}}$ ; (—) predicted by eq 4.

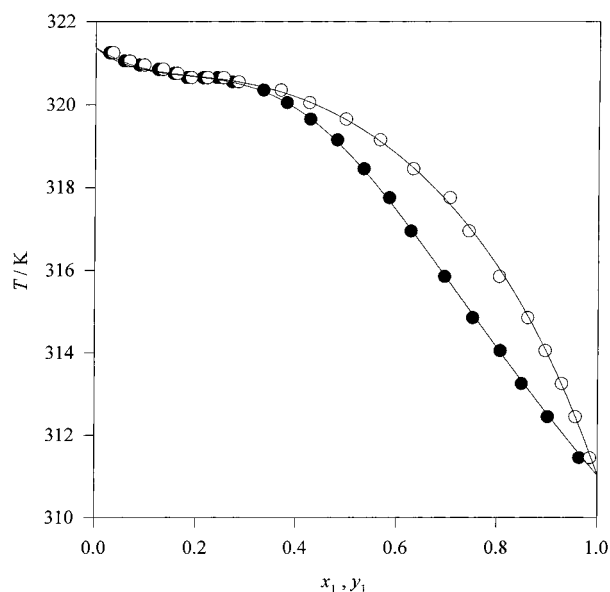


**Figure 5.** Boiling temperature diagram for the system HFC-4310mee (1) + THF (2) at 55.00 kPa: (●) liquid phase mole fraction; (○) vapor phase mole fraction; (—) predicted by eq 4.

where the Antoine constants  $A_i$ ,  $B_i$ , and  $C_i$  are reported in Table 4. It should be pointed out that the experimental vapor pressures were correlated with an average percentage deviation [MADP] of 0.1% for HFC-4310mee and THF. The parameters presented in Table 4 predict very well the experimental vapor pressures reported by Kao et al.<sup>9</sup> for HFC-4310mee [MADP = 0.2%, considering only the data determined by ebulliometry] and by Wu and Sandler<sup>22</sup> for THF [MADP = 0.3%], as can be confirmed in Figure 7. The calculated activity coefficients reported in Table 2 are estimated to be accurate to within  $\pm 3\%$ . The results reported in this table indicate that the system HFC-4310mee (1) + THF (2) deviates negatively from ideal behavior as the concentration of the first component increases. In addition, as shown by Figures 2, 4, and 6, a narrow concentration range exists ( $0 < x_1 < 0.3$ ) where  $\gamma_1 > 1$  and  $\gamma_2 < 1$ , reflecting simultaneous positive and negative deviation from ideal behavior, as required by

**Table 3. Experimental Vapor Pressure Data for Pure Components**

HFC-4310mee		THF	
$T/K$	$P_1^\circ/\text{kPa}$	$T/K$	$P_2^\circ/\text{kPa}$
288.55	20.10	290.25	15.05
291.85	23.59	294.05	17.96
294.45	26.71	297.55	20.98
296.95	29.97	300.65	24.01
300.45	35.12	303.15	26.73
303.65	40.38	305.95	30.04
306.25	45.00	310.25	35.81
308.75	49.93	312.95	39.98
310.75	54.44	315.95	44.95
312.55	58.60	318.75	49.92
314.95	64.49	321.05	54.37
317.05	69.96	323.05	58.57
318.85	75.07	325.95	64.95
320.55	80.08	328.05	69.91
322.25	85.39	330.05	74.93
323.75	90.51	331.85	79.98
325.35	95.85	333.65	84.95
326.85	101.33	335.35	89.92
		337.15	95.46
		338.95	101.33

**Table 4. Antoine Coefficients, Eq 2**

compound	$A_i$	$B_i$	$C_i$
HFC-4310mee <sup>a</sup>	6.438 76	1242.510	46.568
THF <sup>a</sup>	6.148 52	1211.079	46.627

<sup>a</sup> Obtained from the experimental data presented in Table 3.

polyazeotropic behavior. In fact, two azeotropes are present in each isobar at 23.00, 26.68, and 35.00 kPa. These azeotropic concentrations have been estimated by fitting the function

$$f(x_1) = 100 \frac{y_1 - x_1}{x_1} \quad (3)$$

where  $f(x_1)$  is an empirical interpolating function and  $x_1$  and  $y_1$  have been taken from experimental data. Azeotropic concentrations, as determined by solving  $f(x_1) = 0$ , are indicated in Table 5. From the table in question it is concluded that the azeotropic concentrations tend to come

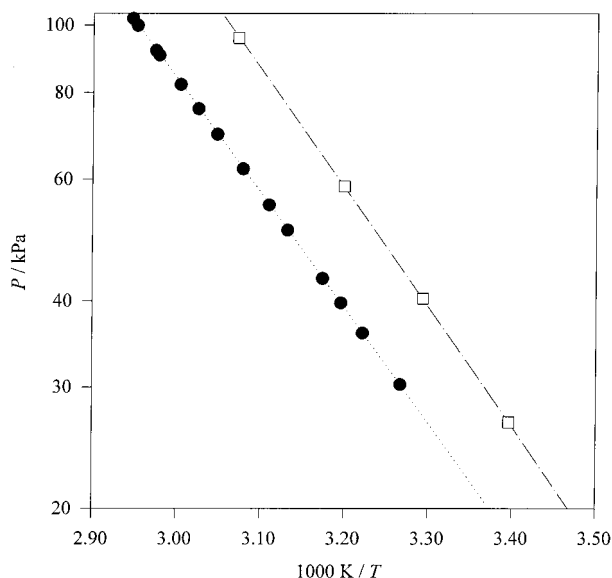


**Figure 7.** Comparison of correlated vapor pressures with other references: experimental data reported by Wu and Sandler<sup>19</sup> for THF (●); experimental data reported by Kao et al.<sup>8</sup> for HFC-4310mee (□); data predicted by eq 2 and parameters given in Table 4 for THF (···) and for HFC-4310mee (– · –).

**Table 5. Polyazeotropic Coordinates for the System HFC-4310mee (1) + THF (2), As Interpolated from Experimental Data**

$P/\text{kPa}$	$x_1^{\text{Az}}, \text{min } T$	$T_{\text{min}}/\text{K}$	$x_1^{\text{Az}}, \text{max } T$	$T_{\text{max}}/\text{K}$
23.00	0.026	299.64	0.312	300.25
26.68	0.047	303.05	0.293	303.45
35.00	0.085	309.40	0.282	309.45

**Table 6. Consistency Test Statistics for the Binary System HFC-4310mee (1) + THF (2)**

system	$N_p^a$	$100\Delta y^b$	$\Delta P^c/\text{kPa}$
26.68 kPa	3	0.5	0.12
35.00 kPa	3	0.5	0.10
55.00 kPa	3	0.4	0.09

<sup>a</sup> Number of parameters for the Legendre polynomial used in consistency. <sup>b</sup> Average absolute deviation in vapor phase mole fractions

$$\Delta y = 1/N \sum_{i=1}^N |y_i^{\text{exptl}} - y_i^{\text{calc}}|$$

( $N$ : number of data points). <sup>c</sup> Average absolute deviation in pressure

$$\Delta P = 1/N \sum_{i=1}^N |P^{\text{exptl}} - P^{\text{calc}}|$$

closer as pressure increases. No azeotrope can be found at (45.00 and 55.00) kPa.

The VLE data reported in Table 2 at (26.68, 35.00, and 45.00) kPa were found to be thermodynamically consistent by the point-to-point method of Van Ness et al.<sup>23</sup> as modified by Fredenslund et al.<sup>24</sup> ( $\Delta y < 0.01$ ). Pertinent consistency statistics are presented in Table 6.

The activity coefficients and the VLE data presented in Table 2 at (26.68, 35.00, and 45.00) kPa were correlated with the Redlich–Kister expansion<sup>25</sup>

$$\frac{G^E}{RT} = x_1 x_2 [C_1 + C_2(x_2 - x_1) + C_3(x_2 - x_1)^2 + C_4(x_2 - x_1)^3] \quad (4)$$

**Table 7. Parameters and Prediction Statistics for Eq 4**

A. Parameters				
$j$	$C_k$			
	$k=1$	$k=4$	$k=3$	$k=4$
0	2.826	0.625	-0.879	0.121
1	-1063.080	-182.011	352.862	0.000

B. Deviation Statistics for Bubble Pressure Calculations		
$P/\text{kPa}$	$100\Delta y$	$\Delta P^a/\%$
26.68	0.4	0.39
35.00	0.5	0.23
55.00	0.3	0.20

$$^a \Delta P\% = 1/N \sum_i^N |P_i^{\text{exptl}} - P_i^{\text{calc}}| / P_i^{\text{exptl}}$$

where the parameters  $C_k$  have been considered temperature-dependent according to

$$C_k = C_k^\circ + \frac{C_k^1}{TK} \quad k = 1, 4 \quad (5)$$

The following objective function (OF) has been used for fitting purposes

$$\text{OF} = \sum_{i=1}^N (|P_i^{\text{exptl}} - P_i^{\text{calc}}| / P_i^{\text{exptl}} + |y_i^{\text{exptl}} - y_i^{\text{calc}}|)^2 \quad (6)$$

and pertinent parameters are reported in Table 7, together with the relative deviation of vapor pressures and the vapor phase mole fraction. No other traditional  $G^E$  model, like NRTL, UNIQUAC, and Wilson (Waldas<sup>26</sup>), has been considered because, on one hand, there is a limited ability of  $G^E$  models to interpolate polyazeotropic data<sup>11</sup> and, on the other hand, none of these traditional models were able to interpolate satisfactorily the complete set of experimental isobars and their activity coefficients. In addition, the model presented in eq 4 predicts well the data of Kao et al.<sup>9</sup> and the partial concentration range data at (23.00 and 45.00) kPa presented in Table 2, as shown in Figure 8.

Figure 8 also depicts the evolution of the polyazeotropic system, as predicted by the model in eq 4. Curve AB corresponds to the locus of the positive deviation azeotropes while curve BC depicts the evolution of the negative deviation ones. As the temperature or the pressure increases, both azeotropes meet the common point B, from which no azeotrope can be found at higher temperatures. Point B was theoretically described the first time by Guminski,<sup>27</sup> who called it a *tangent azeotrope*. In a tangent azeotrope, both the bubble and the dew curves meet a common azeotropic point which, in addition, corresponds to a plane inflection of the equilibrium curve (see line DE in the figure). According to the model in eq 4, the coordinates of the azeotropic point are  $T \sim 314$  K,  $P \sim 42$  kPa, and  $x_1 \sim 0.17$ . The polyazeotropic behavior of the system HFC-4310mee (1) + THF (2) is comparable to the case of the system hexafluorobenzene (1) + benzene (2), which also yields a tangent azeotropic point as the equilibrium pressure increases, as discussed by Ewing et al.<sup>28</sup> Results in Table 5 and the trend of line AB in Figure 8 suggest that the positive deviation azeotrope becomes diluted in HFC-4310mee as temperature decreases below 300 K, so that polyazeotropic behavior *could disappear* at low temperatures, although, due to the operation limitations of our

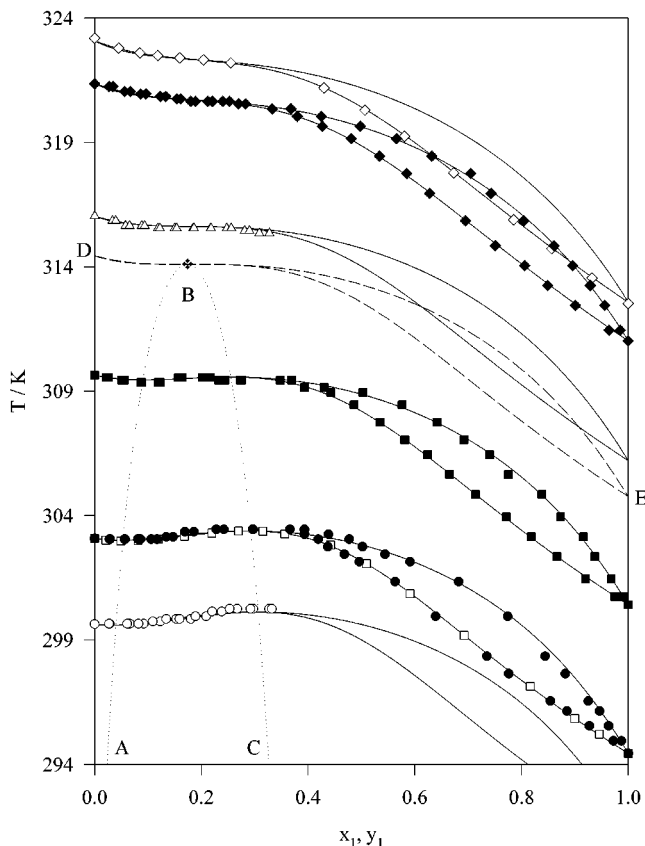


**Figure 8.** Prediction of VLE data: (○) data presented in Table 2 at 23.00 kPa; (□) data of Kao et al.<sup>9</sup> at 26.68 kPa; (●) data presented in Table 2 at 26.68 kPa; (■) data presented in Table 2 at 35.00 kPa; (△) data presented in Table 2 at 45.00 kPa; (◆) data presented in Table 2 at 55.00 kPa; (◇) data of Kao et al.<sup>9</sup> at 58.58 kPa; (—) data predicted by eq 4; (···) polyazeotropic envelope predicted by eq 4; (the diamond located directly above B) tangent azeotropic point predicted by eq 4; (---) tangent azeotrope isobar predicted by eq 4.

apparatus, we do not have experimental data for supporting such an hypothesis.

### Acknowledgment

The authors acknowledge Dr. Chien-Ping Chai Kao, E. I. DuPont de Nemours and Company, who provided the HFC-4310mee used for carrying out this experimental research.

### Literature Cited

- Gaw, W. J.; Swinton, F. L. Thermodynamic Properties of Binary Systems Containing Hexafluorobenzene. Part 4. Excess Gibbs Free Energies of the Three Systems Hexafluorobenzene + Benzene, Toluene, and *p*-Xylene. *Trans. Faraday Soc.* **1968**, *64*, 2023–2034.
- Srivastava, R.; Smith, B. D. Total Pressure Vapor-Liquid Equilibrium Data for Binary Systems of Diethylamine with Acetone, Acetonitrile and Methanol. *J. Chem. Eng. Data* **1985**, *30*, 308–313.
- Aucejo, A.; Loras, S.; Muñoz, R.; Wisniak, J.; Segura, H. Phase Equilibria and Multiple Azeotropy in the Associating System Methanol + Diethylamine. *J. Chem. Eng. Data* **1997**, *42*, 1201–1207.
- Aucejo, A.; Montón, J. B.; Muñoz, R.; Wisniak, J. Double Azeotropy in the Benzene + Hexafluorobenzene System. *J. Chem. Eng. Data* **1996**, *41*, 21–24.
- Leu, A. D.; Robinson, D. B. Vapor-Liquid Equilibrium in Selected Binary Systems of Interest to the Chemical Industry. In *Experimental Results for Phase Equilibria and Pure Components Properties*; Cunningham, J. R., Jones, D. K., Eds.; DIPPR Data Series 1; DIPPR: New York, 1991.
- Christensen, S.; Olson, J. Phase Equilibria and Multiple Azeotropy in the Acetic Acid-Isobutyl Acetate System. *Fluid Phase Equilib.* **1992**, *79*, 187–199.
- Burguet, M. C.; Montón, J. B.; Muñoz, R.; Wisniak, J.; Segura, H. Polyazeotropy in Associating Systems: The 2-Methylpropyl Ethanoate + Ethanoic Acid System. *J. Chem. Eng. Data* **1996**, *41*, 1191–1195.
- Kao, C.; Paulaitis, M.; Yokozeki, A. Double Azeotropy in Binary Mixtures of NH<sub>3</sub> and CHF<sub>2</sub>CF<sub>3</sub>. *Fluid Phase Equilib.* **1997**, *127*, 191–203.
- Kao, C.; Miller, R. N.; Sturgis, J. F. Double Azeotropy in Binary Mixtures 1,1,2,3,4,4,5,5,5-Decafluoropentane + Tetrahydrofuran. *J. Chem. Eng. Data* **2001**, *46*, 229–233.
- Montón, J. B.; Burguet, M. C.; Muñoz, R.; Wisniak, J.; Segura, H. Nonazeotropy in the System Methyl Ethanoate + 1,2-Epoxybutane. *J. Chem. Eng. Data* **1997**, *42*, 1195–1200.
- Wisniak, J.; Segura, H.; Reich, R. Polyazeotropy in Binary Systems. *Ind. Eng. Chem. Res.* **1996**, *35*, 3742–3758.
- Segura, H.; Wisniak, J.; Aucejo, A.; Muñoz, R.; Montón, J. B. Polyazeotropy in Binary Systems. 2. Association Effects. *Ind. Eng. Chem. Res.* **1996**, *35*, 4194–4202.
- van Konynenburg, P.; Scott, R. L. Critical lines and phase equilibria in binary van der Waals mixtures. *Philos. Trans. R. Soc. (London)* **1980**, *298A*, 495–539.
- Segura, H.; Wisniak, J.; Toledo, P. G.; Mejía, A. Prediction of Azeotropic Behavior Using Equations of State. *Fluid Phase Equilib.* **1999**, *166*, 141–162.
- Merchant, A. N.; Minor, B. H. PCT Int. Appl., **1999**.
- Michaud, P.; Martin, J.-J. Eur. Pat. Appl., **1998**.
- Merchant, A. N.; Minor, B. H.; Molyadim, S. A. PCT Int. Appl., **1997**.
- Van Ness, H. C.; Abbott, M. M. *Classical Thermodynamics of Nonelectrolyte Solutions*; McGraw-Hill Book Co.: New York, 1982.
- Tripp, T. B.; Dunlap, R. D. Second Virial Coefficients for the Systems: Butane + Perfluorobutane and Dimethyl Ether + 1-Hydroperfluoropropane. *J. Phys. Chem.* **1962**, *66*, 635–639.
- Garner, M. G. D.; McCoubrey, J. C. Second Virial Coefficients of Hydrocarbon + Fluorocarbon Mixtures. *Trans. Faraday Soc.* **1959**, *55*, 1524–1530.
- Hossenlopp, I. A.; Scott, D. W. Vapor Heat Capacities and Enthalpies of Vaporization of Six Organic Compounds. *J. Chem. Thermodyn.* **1981**, *13*, 405–414.
- Wu, H. S.; Sandler, S. I. Vapor-Liquid Equilibria of Tetrahydrofuran Systems. *J. Chem. Eng. Data* **1988**, *33*, 157–162.
- Van Ness, H. C.; Byer, S. M.; Gibbs, R. E. Vapor-Liquid Equilibrium: Part I. An Appraisal of Data Reduction Methods. *AIChE J.* **1973**, *19*, 238.
- Fredenslund, A.; Gmehling, J.; Rasmussen, P. *Vapor-Liquid Equilibria Using UNIFAC*; Elsevier: Amsterdam, 1977.
- Redlich, O.; Kister, A. T. Algebraic Representation of Thermodynamic Properties and the Classification of Solutions. *Ind. Eng. Chem.* **1948**, *40*, 345–348.
- Walas, S. M. *Phase Equilibria in Chemical Engineering*; Butterworth Publishers: Boston, 1985.
- Guminski, K. Z. Rozwazan Nad Punktem Azeotrowym. *Rocz. Chem.* **1958**, *32*, 569–582.
- Ewing, M.; Kimpton, S.; McGlashan, M. Limited Azeotropy in Fluid (Benzene + Hexafluorobenzene). *J. Chem. Thermodyn.* **1984**, *16*, 669–671.
- Ramkumar, D. H. S.; Odak, S. V.; Kudchadker, A. P. Mixture Properties of the Water +  $\gamma$ -Butyrolactone + Tetrahydrofuran System. 3. Isobaric Vapor-Liquid Equilibrium of Water +  $\gamma$ -Butyrolactone and Tetrahydrofuran +  $\gamma$ -Butyrolactone at 1.013 bar. *J. Chem. Eng. Data* **1989**, *34*, 459–463.

Received for review March 13, 2001. Accepted June 8, 2001. This work has been partially financed by FONDECYT, Chile, Project No. 1990402.

JE0100793